ELSEVIER

Biophysical Chemistry 120 (2006) 1 – 9

Biophysical Chemistry

http://www.elsevier.com/locate/biophyschem

A comparison between two prokaryotic potassium channels (KirBac1.1 and KcsA) in a molecular dynamics (MD) simulation study

Mikko Hellgren [a,c], Lars Sandberg [b], Olle Edholm [a,*]

[a] *Theoretical Biological Physics, Department of Physics, Royal Institute of Technology, AlbaNova University Centre, SE-106 91 Stockholm, Sweden*
[b] *AstraZeneca R and D Mölndal SE-431 83 Mölndal, Sweden*
[c] *Department of Medical Biochemistry and Biophysics, Karolinska Institute, SE-171 77 Stockholm, Sweden*

Received 19 August 2005; received in revised form 3 October 2005; accepted 3 October 2005
Available online 25 October 2005

Abstract

The two potassium ion channels KirBac1.1 and KcsA are compared in a Molecular Dynamics (MD) simulation study. The location and motion of the potassium ions observed in the simulations are compared to those in the X-ray structures and previous simulations. In our simulations several of the crystallography resolved ion sites in KirBac1.1 are occupied by ions. In addition to this, two in KirBac1.1 unresolved sites where occupied by ions at sites that are in close correspondence to sites found in KcsA. There is every reason to believe that the conserved alignment of the selectivity filter in the potassium ion channel family corresponds to a very similar mechanism for ion transport across the filter. The gate residues, Phe146 in KirBac1.1 and Ala111 in KcsA acted in the simulations as effective barriers which never were passed by ions nor water molecules.

Keywords: Potassium channel; Molecular dynamics simulation; KcsA; KirBac1.1

1. Introduction

The conduction of ions across cell membranes is of central importance for a wide range of physiological functions. Potassium ion channels control the electric potential across the cell membrane by catalysing rapid, transport of potassium ions along an electro-chemical gradient [1,2]. All potassium ion channels are tetramers with several conserved secondary structural elements. KcsA and KirBac1.1 are two prokaryotic potassium ion channels with known crystal structures [1,3]. The most recently resolved potassium channel is KirBac3.1, which gives us in total five potassium ion channels (KcsA, KirBac1.1, KirBac3.1, KvAP, MthK) with known structure. All five are from prokaryotic species. Kir stands for potassium (K) inward rectifying and proteins of this class are important for regulation of membrane excitability, vascular tone, insulin release and salt flow across epithelia [3]. Inward rectification is caused by cytoplasmic ligands (Mg^{2+} and polyamines), the binding sites of which are unknown in KirBac1.1 but were resolved in the KirBac3.1 crystal structure which contains sites occupied by Mg^{2+} and spermine. The prokaryotic potassium ion channel KirBac1.1 is closely related to the eukaryotic Kir potassium ion channels [4,5].

Potassium ion channels remove the hydration shell from the ion when it enters the selectivity filter. The selectivity filter is formed by five residues (TVGYG) from each subunit which have their electro-negative carbonyl oxygen atoms aligned towards the centre of the filter pore and form an anti-prism similar to a water solvating shell around each potassium binding site. The distance between the carbonyl oxygens and potassium ions in the binding sites of the selectivity filter is the same as between water oxygens in the first hydration shell and a potassium ion in water solution. The selectivity filter opens towards the extracellular solution, exposing four carbonyl oxygens in a glycine residue (Gly79 in KcsA and Gly114 in KirBac1.1). The next residue towards the extracellular side of the protein is the negatively charged Asp80 (KcsA)/Asp115(KirBac1.1). This residue form together with the five filter residues the pore that connects the water filled cavity in the centre of the protein with the extracellular solution. The

* Corresponding author. Tel.: +46 8 55378168; fax: +46 8 55378216.
E-mail address: oed@theophys.kth.se (O. Edholm).

0301-4622/$ - see front matter © 2005 Elsevier B.V. All rights reserved.
doi:10.1016/j.bpc.2005.10.002

carbonyl oxygens are strongly electro-negative and cation attractive. The filter can accommodate potassium ions at 4 sites usually labelled S1 to S4 starting at the extracellular side. In addition one ion can bind in the cavity at a site that we will label SC and one or more ions at the extracellular side at more or less well defined sites labelled S0 or Sext. Several different occupancies of these sites are possible. Since the X-ray structures are averages over many molecules, it is, however, not possible to deduce the actual occupancies directly from such a structure. In general, there is some disadvantage due to electrostatic repulsion to have two neighbouring sites occupied by ions. The mechanism for ion translocation in KcsA has been studied extensively by simulation techniques [6–8]. See also the reviews [9,10]. A complete map of the free energies of the $2^4=16$ states (characterised by the occupancy of the S1, S2, S3 and S4 sites) was calculated in Ref. [6] resulting in the prediction of an ion conduction mechanism in which the two doubly occupied states (S1, S3) and (S2, S4) play an essential role. A similar view was also advocated in Ref. [11] based on experimental evidence. The two extracellular states, Sext and S0, were found in a better resolved structure of KcsA at high potassium concentration [1]. In free energy calculations [8] the entire ionic pathway from the cavity, through the four filter sites out to S0 and Sext was covered.

The amino acids sequence of the selectivity filter of potassium ion channels is conserved with the exception that an isoleucine residue in eukaryotic potassium ion channels often is substituted with a valine residue in prokaryotic channels. KcsA and KirBac1.1 have a valine (V76/V111) while KirBac3.1 is exceptional for prokaryots by having an isoleucine (I97) in this position. The secondary structure of the residues close to the selectivity filter is also believed to be conserved while the gate and the cytoplasmic part of are not that well conserved. This can be seen in a comparison of KirBac1.1 with KcsA. The former has a large cytoplasmic part (about 180 residues) while KcsA only has about 40 residues on the cytoplasmic side of the membrane. The sequence alignment of KirBac1.1, KirBac3.1 and KcsA can be seen in Fig. 1. The alignment shows that the most conserved part of the proteins is the region labelled the pore region (which includes a short helix and the selectivity filter motif, TVGYG). This part is also characterised by small temperature factors and a small root mean square deviation (about one Å) between the positions of the C_α atoms in the different crystal structures. The region named the slide helix in the KirBac structures is a short amphipatic helix that lies in the membrane interface. This region is not crystalographically resolved for KcsA, but there are some evidences of a helix conformation similar to that of the KirBac channels [12]. Our alignment does, however, not indicate a strong evolutionary similarity in this region, even if the amphipathicy is equally pronounced in both cases.

The ion channels have two different conformations corresponding to an open and a closed state. The crystal structures of KcsA as well as KirBac1.1 are believed to be closed. It has, however, been proposed that KcsA is an open channel with a closed gate while KirBac1.1 is a closed channel with a closed gate [3]. Site-directed spin labelling (SDSL) and electron paramagnetic resonance (EPR) spectroscopy studies of KcsA have, however, revealed some features of the open structure of KcsA. The positions of the C_α atoms of the inner helix in KcsA (residues 86–119) that forms the lining of the gate have been determined in the open state (pdb entries 1JQ1 and 1JQ2) [13]. The channel is opened by a rotation of the *trans*-membrane alpha helices which increase the distance between the C_α:*s* of the helices at the narrowest part of the gate (Ala111) by 0.3 nm. The open conformation of KcsA and KirBac3.1 (pdb entry

PROTEIN	SLIDEHELIX	TURN	OUTERHELIX
Alignment	/ */* *	*	#*** / # # *+***#+*++
KirBac1.1	47VWRDLYYWALK57	58VS59	60WPVFFASLAALFVVNNTLFALLYQL84
KirBac3.1	33WLDDHYHDLLT43	44VS45	46WPVFITLITGLYLVTNALFALAYLA70
KcsA	13VKLLLGRHGSA23	24LH25	26WRAAGAATVLLVIVLLAGSYLAVLAE51

PROTEIN	EXTRACELLULAR	PORE
Alignment	#*//*/* *	* #***##/# *#/###/+ #
KirBac1.1	85GDAPIANQSPP95	96GFVGAFFFSVETLATVGYGDMHP118
KirBac3.1	71CGDV-IENARPG81	82SFTDAFFFSVQTMATIGYGKLIP104
KcsA	52RG-APGAQLI60	61TYPRALWWSVETATTVGYGDLYP83

PROTEIN	TURN	INNERHELIX
Alignment	/	* /*** #* * */ / * **#
KirBac1.1	119QT120	121VYAHAIATLEIFVGMSGIALSTGLVFARF149
KirBac3.1	105IG106	107PLANTLVTLEALCGMLGLAVAASLIYARF135
KcsA	84VT85	86LWGRCVAVVVMVAGITSFGLVTAALATWF114

Fig. 1. Alignment of the sequences of three potassium channels, KirBac1.1, KirBac3.1 and KcsA. # denotes an amino acid that is conserved between all three structures, * an amino acid conserved between KirBac1.1 and KirBac3.1, / an amino acid conserved between KirBac1.1 and KcsA while + denotes an amino acid conserved between KirBac3.1 and KcsA.

1XL6) show that large inorganic cations and inactivation peptides can enter the pore from the intracellular solution. These inhibitors stop the conduction of potassium ions by directly blocking the ion permeation path and compete with ions for binding sites within or close to the channel pore [14–16].

2. Simulation and alignment procedures

The alignment between the three potassium channels shown in Fig. 1 is based on aligning the different secondary structural elements observed in the crystal structures. There is then an uncertainty of a couple of residues about exactly where to set the borderline between any two regions. We have chosen to divide the sequence into five main structural elements, the slide helix, the outer helix, an extracellular part, the pore (consisting of a short helix and the selectivity filter) and the inner helix with in some cases short links between the elements. For each of these region a score function (Score) that measures the degree of similarity between the three sequences has been calculated. This function is defined to be 1 for perfectly matching sequences and the more close to zero the more dissimilar the sequences are. We chose the following definition:

$$\text{Score} = \frac{1}{N}\sum_{i=1}^{N}\frac{s_i}{3} \quad (1)$$

were the sum goes over all N residues in the aligned part of the sequence and s_i is the number of matchings for residue i. This number is 3 when all sequences match, 1 if two of them match and 0 if none of them match. There is no punishment for the few gaps in the alignment, but they are just ignored. The result is presented in Table 1.

All simulations were performed using the parallel version of the GROMACS package [17–19] on a small cluster of dual-Pentium machines running Linux. An effort was made to chose all parameters and setups in the simulation of the two channels as equal as possible. All systems were subject to periodic boundary conditions in all directions. The temperature was kept constant at 300 K using separate Berendsen thermostats [20] for protein, water, ions and lipids with the time constants 0.1 ps. The pressure was coupled to a Berendsen barostat with pressure 1 atm separately in the three spatial directions, using a time constant of 5 ps. The integration of the equations of motion was performed using a leap frog algorithm with a time step of 2 fs. A cutoff 1.0 nm was used for the Lennard–Jones (LJ) interactions while the electrostatic interactions were calculated using the Particle Mesh Ewald (PME) method [21,22] outside a cutoff 1.0 nm. The system included protein, dipalmiotylphosphatidylcholin (DPPC) lipids, water, potassium and chloride ions. The standard GROMACS potential parameters in the united atom force field (non-polar hydrogens included with carbons into united hydrocarbon groups) were used as far as possible. The DPPC lipids were modelled with the parameters described in Ref. [23] which reproduces experimental properties of lipid bilayers well, including areas per lipid. It should be noted that the temperature, 300 K, is below the gel/liquid crystalline phase transition temperature. Still the lipids did remain in the high temperature phase during the entire simulation. There are two reasons for this, first a transition would require considerably longer time than the order of 10 ns that our simulations covered. Further, the perturbing influence exerted by the protein on the fairly small number of lipids included in the simulation may significantly alter the phase transition properties of the lipids. For the water we used the SPC model [24], bonds and angles held constant using the analytical SETTLE method [25]. For the potassium and chloride ions the standard Lennard–Jones parameters of the GROMACS force field were used.

Only the membrane spanning part of the proteins were included in the simulations. This corresponds to residues Ala23–Gln149 for the KcsA channel, which are the residues that were available in the first X-ray structure (pdb entry 1BL8). In later structures a few additional residues have been resolved. In KirBac1.1 we excluded the unresolved N-terminus but also the 10 resolved residues (36–45) which extend out into the water and form a flexible linker. This means that we start with Ser46 which is the first residue of the amphipathic 'slide' helix (Ser46–Arg57). On the C-terminal side KirBac1.1 contains a large (180 residues of which about 140 were resolved in the X-ray structure) intracellular part (the vestibule) which we also excluded in the simulation. It was, however, not obvious where to make the cut. We made the choice to stop at Ala150 despite that this makes the protein is a couple of residues shorter on the C-terminal side in the KirBac1.1 simulation as compared to the KcsA simulation. The reason was that three of the consecutive five residues can be positively charged depending on protonation. There are also residues belonging to parts in the vestibule much further down in the sequence that are close in space and can be negatively charged depending on protonation. Therefore, the inclusion of residues beyond Ala150 would in our opinion have created too much uncertainties in the modelling to justify the possible small improvement. The choice of protonation state for all residues in the proteins was not evident. We applied the protonation state the amino acid would have in water solution at pH 7 except for a couple of deeply buried residues. These exceptions were Glu106 in KirBac1.1 which corresponds to Glu71 in KcsA and Glu130 in KirBac1.1 which have no counterpart in KcsA which all were taken protonated and neutral. The protonated neutral state of Glu71/Glu106 is in agreement with results from accurate free energy integrations on KcsA [26,27] but at variance with having a proton shared between Glu71 and Asp80 in KcsA and between Glu106 and Asp 115 in KirBac1.1

Table 1
The scores for different parts of the structure calculated from Eq. (1) for the alignment of the sequences of KcsA, KirBac1.1 and KirBac3.1 shown in Fig. 1

Part of the protein	Number of residues	Score
Slide helix	11	0.15
Outer helix	25	0.33
Extracellular	9	0.37
Pore	23	0.52
Inner helix	29	0.22

advocated in Ref. [28]. The choice of a neutral protonated Glu130 is in agreement with Ref. [28]. The different structural elements, alignment and protonation is shown schematically in Table 2. The C- and N-termini were protonated and unprotonated, respectively to become neutral.

The systems were prepared and equilibrated in the following way. For the lipid bilayer an equilibrated system containing 256 lipids was employed. A number of lipids were removed from the bilayer in such a way that a cylindrical hole was created in which the protein would fit. To do this, it was necessary to remove about 70 lipids corresponding to an area of 22 nm^2. Since the proteins have conical shape a different number of lipids was removed from the two sides of the lipid bilayer. For KcsA, we removed 37 lipids from the side of the bilayer at which the thicker (extracellular) end of the protein would be located and 33 lipids from the other side of the bilayer. KirBac1.1 is a bit larger and less conical due to the slide helices. In total 74 lipids were removed in that system. These systems were then solvated in water. The cavities in the two channels are different in size. We decided for 24 waters in the KcsA cavity and 20 waters in the smaller KirBac1.1 cavity. The simulations were started with potassium ions initially in the S2, S4 and SC positions inside the protein. The choice of protonation gives with 3 potassium ions in the channel a net charge of plus three electron charges for the KirBac1.1 tetramer and minus one for the KcsA tetramer. In addition to these ions we added potassium and chloride ions at randomly selected positions in the water solution to obtain a totally electro neutral system with a concentration of around 100 mM for both ion types. This is fairly similar to the concentrations in biological organisms which, however, have different intra- and extracellular ionic concentrations. In a frog muscle cell, the intracellular potassium ion concentration is about ten times higher than the extracellular potassium ion concentration and for chloride ions the reverse relation holds. In a bilayer simulation that uses periodic boundary conditions we can, however, not distinguish between an intra- and an extracellular water solution. In this way we ended up with the number of molecules and atoms according to Table 3.

The systems were then energy minimised and equilibrated in successive molecular dynamics simulations extending up to 3 ns in total with the protein coordinates strongly restrained to the pdb structure. These equilibrations were first run at constant volume then at constant pressures in all three directions to allow the system to adjust its density and area to thickness ratio. Some waters in the hydrophobic region between the protein and the lipids were removed in the middle of this equilibration procedure. When the bilayer structure and water around the protein had stabilised after these equilibrations, the restraints on the protein were successively released and another nanosecond of equilibration followed. After this we started one 5 ns simulation for KcsA and two 5 ns simulations with KirBac1.1. This is sufficient to study the (meta) stable equilibrium situation with the internal ions close to their initial positions. It is, however, not at all sufficient for studying transport or true equilibrium between the different ion occupancies. Even though the ion permeation rate for KirBac1.1 is unknown, a reasonable estimate for the average ion passage time is about 30 ns for an open running channel [28]. For that purpose simulations that are several orders of magnitude longer (and not possible with present computer technology) are necessary or more elaborate techniques like free energy perturbation that moves the ions between different sites.

Table 3
The number of molecules and atoms included in the simulations

	KcsA		KirBac1.1	
	Molecules	Atoms	Molecules	Atoms
Protein	4	3704	4	4228
Lipid	186	9300	182	9100
Water	9841	29,523	9858	29,574
K^+	14	14	18	18
Cl^-	22	22	18	18
Total		42,563		42,938

3. Results and discussion

The main results from the simulations are illustrated in molecular graphics form in Fig. 2 and as positions of ions and some important residues in Fig. 3 for the KcsA simulation and in Fig. 4a and b for the two simulations of the KirBac1.1 channel. In these figures, we have centred the protein and the ions with respect to the average positions of the five filter

Table 2
The alignment and protonation of some residues (potentially charged and residues that forms a boundary between different secondary structural elements) included in the simulations of KcsA and KirBac1.1

	Slide helix				Turn		Outer helix			Loop	
KirBac1.1	V47	$R49^+$	$D50^-$	$K57^+$	V58	S59	W60	P61	L84	G85	$D86^-$
KcsA				A23	L24	H25	W26	$R27^+$	$E51^-$	$R52^+$	G53
Loop	Short helix				Selectivity filter						
P95	G96	G99	E106	A109	T110	V111	G112	Y113	G114	$D115^-$	P118
I60	T61	$R64^+$	E71	T74	T75	V76	G77	Y78	G79	$D80^-$	P83
Turn		Inner helix									
Q119	T120	V121	H124	E130	F146	$R148^+$	F149	A150			
V84	T85	L86	$R89^+$	V95	A111	W113	F114	V115	$K117^+$	$E118^-$	Q119

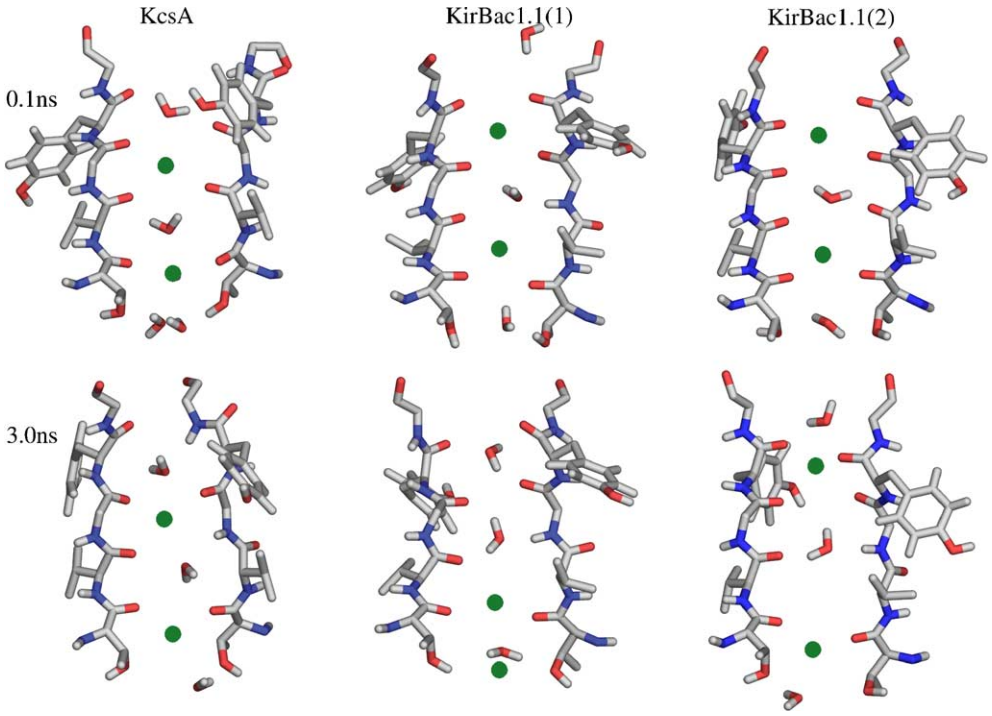

Fig. 2. Two snapshots of the selectivity filter (the TVGYG motif) and potassium ions and water inside it from each of the three simulations. The first row is taken after 0.1 ns and the second after 3 ns. The left column is from the KcsA simulation with the S2 and S4 ions, the middle one from the first KirBac1.1 simulation with the S1 and S3 ions at 0.1 ns and the S3-4 and SC ions at 3 ns while the right column is from the second KirBac1.1 simulation with the S1 and S3 ions at 0.1 ns and the S1 and S4 ions at 3 ns.

residues in the four monomers. Thus, we can accurately compare ion positions in the two channels with each other and between simulations and X-ray structures.

It has become evident both from simulation studies [26,9] and available crystal structure data [1,29] that the ion occupancy in the KcsA selectivity filter is about 2 at high potassium concentration. The two potassium ions have an almost uniform distribution over four equally spaced ion-binding sites (S1 to S4) corresponding to two distinct configurations; the S1/S3 configuration and the S2/S4 con-

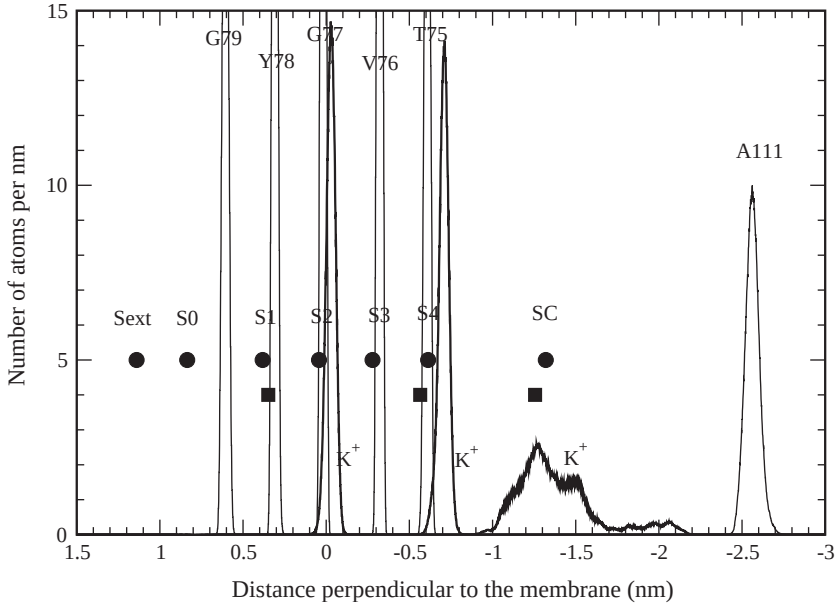

Fig. 3. The distribution of the potassium ions inside the KcsA channel during 5 ns of simulation versus the coordinate along the ion channel. In addition the distributions of the C_α atoms of the five filter residues (Thr75, Val76, Gly77, Tyr78 and Gly99) are shown (thin lines). The 7 black circular dots show the potassium positions in the crystal structure (pdb entry 1K4C) while the 3 squares show the corresponding positions in the low potassium concentration structure (1K4D). The potassium ions of the simulation are in the sites labelled S2, S4 and SC. In addition the distribution of the C_α atoms of the four Ala111 residues which are located at the most narrow part of the entrance from the intracellular side is shown.

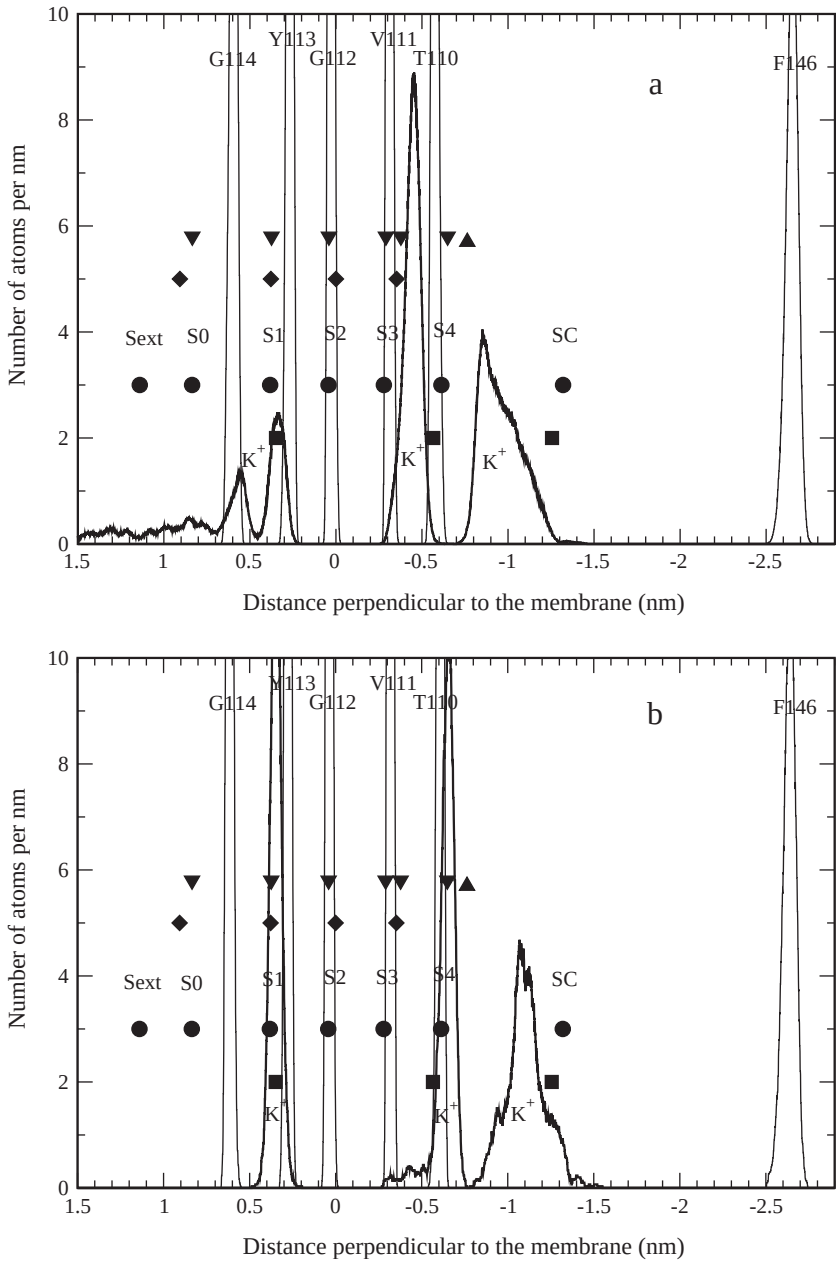

Fig. 4. The distribution of the potassium ions inside the KirBac1.1 channel during the two different 5 ns simulations (a and b) versus the coordinate along the ion channel. In addition the distributions of the C_α atoms of the five filter residues (Thr110, Val111, Gly112, Tyr113 and Gly114) are shown (thin lines). The four diamond dots show the potassium positions in the crystal structure (pdb entry 1P7B). For comparison the 7 potassium positions in the KcsA structure (1K4C) (black dots), the three ionic positions in 1K4D (black squares), the 6 potassium positions in KirBac3.1 (1XL6) (triangle down) and the single magnesium ion (triangle up) are shown. In addition, the distribution of the C_α atoms of the gating residues (Phe146) on the intracellular side is shown.

figuration with water molecules in between the occupied ion sites. However, at low potassium concentrations only one potassium ion, on average, occupy the selectivity filter [1,29]. At the same time the selectivity filter undergoes small conformational changes while the other parts of the ion channel are essentially unchanged. Further, results at low ionic concentration show that the ion distribution is shifted towards position S1 and S4 while S2 and S3 are more or less unoccupied [11].

In the simulation of the KcsA channel, we observe that the S2 and S4 ions remain at these sites. It seems, however clear that their average positions are slightly shifted towards the cavity with about 0.1 nm compared to the positions in the X-ray structure. The distributions are quite narrow with root mean square fluctuation of about 0.03 nm. The cavity ion has on the other hand quite a wide distribution. The root mean square fluctuation is about 0.2 nm for the main part of the distribution. In addition, the ion makes an excursion of about 0.7 nm towards the intracellular entrance at the end part of the simulation. This is not compatible with the X-ray temperature factors which indicate an almost as narrow distribution for the cavity ion as for the ions at the sites in the filter.

In the first KirBac1.1 simulation with an initial S2 and S4 ion configuration, the S2 ion moves very fast during the equilibration to the S1 site. During the 5 ns of simulation, it moves from the S1 site out to the S0 and Sext site and back to S1 after 3.5 ns and stays then in the S1 site 0.2 ns to finally escape out to the extracellular water solution. There is then a tendency to bind for some time close to G114. The motion of the ion is illustrated in Fig. 5. From Fig. 4a we note that while the *S*4 ion ended up about 0.1 nm off from the S4 position in the direction of the cavity in the KcsA simulation we now observe a shift of about 0.15 nm in the opposite direction. This brings the ion in the KirBac1.1 simulation into a position between the S3 and S4 sites of KcsA. We also note that there is no resolved S4 site in the X-ray structure of the KirBac1.1 channel and that the S3 site of this channel is slightly shifted towards the cavity compared to the position in KcsA. If we start from the S3 site in KcsA and move in the directions of the cavity, the following entities follows consecutively: (1) the S3 site in KirBac1.1 after 0.07 nm; (2) the ion in the KirBac1.1 simulation after 0.16 nm; (3) the S4 site of KcsA after 0.34 nm; (4) the S4 ion in the KcsA simulation after in total 0.42 nm.

We also observe that the cavity ion has a wide distribution (but slightly less wide than in KcsA). This distribution is not centred on the cavity site of KcsA but about 0.5 nm closer to the filter. The distribution is not symmetric and drops quite steeply in the direction towards the filter, while is more stretched towards the gate site of the cavity.

During the escape of the S2 ion to the S1 site it spends some time at a well defined site about 0.2 nm outside the S1 site just inside G114. Once the ion has passed G114 the distribution is quite at and we see no evidence of one or more well defined S0 sites.

In a second simulation of KirBac1.1 with an initial S1 and S3 ion configuration, we observe that after 0.5 ns the S3 ion moves to a stable S4 position. This is reflected in the ionic distribution in Fig. 4b which has main peak at the S4 site but a part of the distribution reflecting the first 0.5 ns around the S3 site. This conformation is maintained throughout the rest of the simulation. The ion distribution of the cavity ion is compared to the first simulation of KirBac1.1 slightly shifted towards the centre of the cavity (away from the selectivity filter) but still centred closer to the filter than in KcsA.

The final position of the S4 ion in the first KirBac1.1 simulation is stabilised by the carbonyl oxygens of both T110 and V111. In the KcsA simulation, and the second KirBac1.1 simulation the ionic position is shifted more toward the proper S4 site and the ion is stabilised by interactions the threonine carbonyls and the oxygens of the threonine side chains but not with the valine carbonyl oxygens. The reasons for this difference may be complex. The close proximity between the cavity ion and the S4 site together with the large distance to the next ion on the extracellular side could favour the extracellular shift of the S4 ion position in the direction of the S3 site.

The KirBac1.1 channel remained closed at the intracellular entrance by four Phe146 residues in both simulations. The Phe146 residues had their side-chains of aromatic rings pointing inward and by this stopped the entrance/exit of ions. The gate (Phe146) in KirBac1.1 is in its closed state an effective barrier that stop molecules to enter or leave the cavity. In KcsA the most narrow part of the channel towards the intracellular side is the four Ala111 residues. No ions and no water molecules passed the Ala111/Phe146 residues during the simulations. From the alignment in Fig. 1 we observe that the residue Phe146 (gate-residue) in KirBac1.1 corresponds to Tyr132 residue in KirBac3.1 and Ala111 in KcsA. These three residues form to the most narrow part of the ion channels opening towards the intracellular side. This indicates a conserved relative position for the proposed gate residue in the potassium ion channel family. Table 1 shows the scores

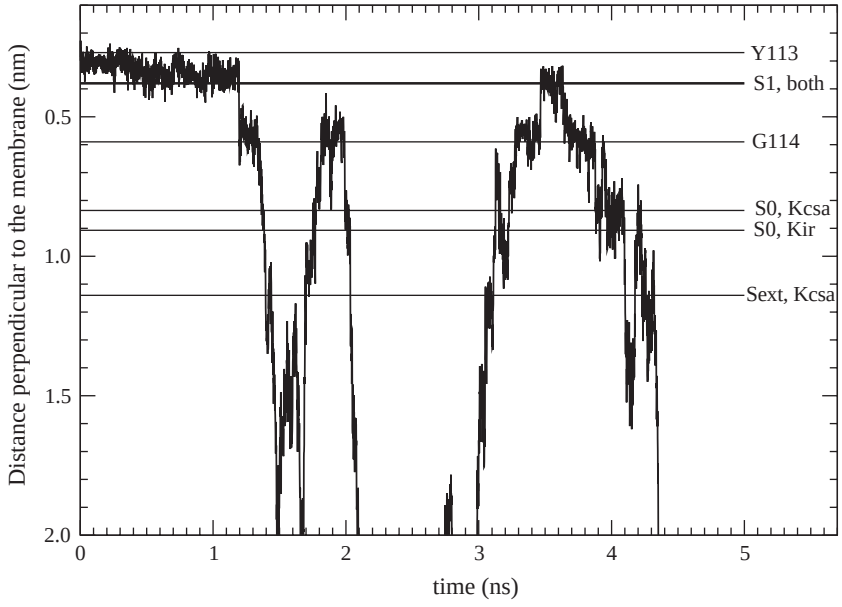

Fig. 5. The *z* coordinate of the S0/S1 ion in the first KirBac1.1 simulation during versus time.

from the alignment shown in Fig. 1. It is obvious that the pore region is the most conserved part of the proteins and that the function Score drops with distance from this region. The two membrane spanning helices (outer- and inner-helix) of each subunit of the potassium channels are to a lesser extent conserved. The cytoplasmic region is not conserved and this is probably related to differences in regulation of the gating.

4. Conclusions

The main difference between the present KirBac1.1 simulations and those of Domene et al. [28] is that we include a cavity ion. Further, we have less water, 20 instead of 27 in the cavity and there is a minor difference in the protonation state of the channel monomer (see above). The initial ion conformations were also chosen differently. We start in the KcsA simulation and in the first KirBac1.1 simulation with the two selectivity filter ions in the S2 and S4 sites with a water in between, while they start with them in the S1 and S3 sites. Our second simulation of KirBac1.1 is similar to that in Ref. [28] but it includes a cavity ion. The ions in the simulations of Ref. [28] move very fast into stable final conformations and they show that this occurs in less than 0.5 ns. We do also observe changes occurring on these time scales but also changes over longer time scales. We observe a stable S2/S4/SC ion conformation in the KcsA simulation. In the first KirBac1.1 simulation we find a stable S3–4/SC ion conformation and in the second simulation of KirBac1.1 a stable S1/S4/SC ion conformation. Hence, both of our simulations of KirBac1.1 were started in configurations corresponding to a high potassium ion concentration, but end up in configurations similar to a low ion concentration.

All this indicates that many extensive simulations would be necessary to fully explore all complex possibilities for distributing different numbers of ions in the filter region. The main conclusions from the present simulations are: The ion distribution in the cavity may be quite wide. We see a 2 Å shift in the distribution towards the selectivity filter of the ion occupancy in KirBac1.1 compared to KcsA. When the potassium ion occupy the S3/S4 position it coordinates to the carbonyl groups of Val and Thr. However, when the ion resides in the S4 site it coordinates to the carbonyl groups and the hydroxyl groups of the same Thr residues. The potassium ion in the S1 site can reversibly move both to S0, Sext and further out in the solution on the extracellular side of the membrane on the simulation time scales and we observe no well defined S0 or Sext sites in KirBac1.1 in the simulations. In the present work, a distribution with ions in the S2 and S4 sites corresponding to what would be the most stable state at high potassium concentration remains stable in the KcsA simulation. In the KirBac1.1 simulations on the other hand the final states are either a singly occupied state between the S3 and S4 states or a state with ions in the S1 and S4 sites. Hence, we suggest, based on the results of our simulation study, that the KirBac1.1 structure is in a low K^+ solution conformation. This is in accordance with the fact that KirBac1.1 is a closed channel with a closed gating section.

References

[1] Y. Zhou, J.H. Morais-Cabral, A. Kaufman, R. Mackinnon, Chemistry of ion coordination and hydration revealed by a K^+ channel-Fab complex at 2.0 Å resolution, Nature 414 (2001) 43–48.
[2] Y. Jiang, A. Lee, J. Chen, M. Cadene, B.T. Chait, R. MacKinnon, Crystal structure and mechanism of a calcium-gated potassium channel, Nature 417 (2002) 515–522.
[3] A. Kuo, J.M. Gulbis, J.F. Antcliff, T. Rahman, E.D. Lowe, J. Zimmer, J. Cuthbertson, F.M. Ashcroft, T. Ezaki, D.A. Doyle, Crystal structure of the potassium channel KirBac1.1 in the closed state, Science 300 (2003) 1922–1926.
[4] D. Bichet, F.A. Haass, L.Y. Jan, Merging functional studies with structures of inward-rectifier K^+ channels, Nat. Rev., Neurosci. 4 (2003) 957–967.
[5] S.R. Durell, H.R. Guy, A family of putative Kir potassium channels in prokaryotes, BMC Evol. Biol. 1 (2001) 14.
[6] J. Åqvist, V. Luzhkov, Ion permeation mechanism of the potassium channel, Nature 404 (2000) 881–884.
[7] S. Berneche, B. Roux, Energetics of ion conduction through the K^+ channel, Nature 414 (2001) 73–77.
[8] S. Berneche, B. Roux, A microscopic view of ion conduction through the K^+ channel, Proc. Natl. Acad. Sci. U. S. A. 100 (2003) 8644–8648.
[9] B. Roux, Theoretical and computational models of ion channels, Curr. Opin. Struct. Biol. 12 (2002) 182–189.
[10] V. Luzhkov, J. Åqvist, Ions and blockers in potassium channels: insights from free energy simulations, Biochim. Biophys. Acta 1747 (2005) 109–120.
[11] J.H. Morais-Cabral, Y. Zhou, R. MacKinnon, Energetic optimization of ion conduction rate by the K^+ selectivity filter, Nature 414 (2001) 37–42.
[12] D.M. Cortes, L.G. Cuello, E. Perozo, Molecular architecture of full length KcsA: role of cytoplasmic domains in ion permeation and activation gating, J. Gen. Physiol. 117 (2001) 165–180.
[13] Y.S. Liu, P. Sompornpisut, E. Perozo, Structure of the KcsA channel intracellular gate in the open state, Nat. Struct. Biol. 8 (2001) 883–887.
[14] Y. Jiang, A. Lee, J. Chen, M. Cadene, B.T. Chait, R. MacKinnon, The open pore conformation of potassium channels, Nature 417 (2002) 523–525.
[15] V.B. Luzhkov, J. Åqvist, Mechanisms of tetraethylammonium ion block in the KcsA potassium channel, FEBS Lett. 495 (2001) 191–196.
[16] M. Zhou, J.H. Morais-Cabral, S. Mann, R. Mackinnon, Potassium channel receptor site for the inactivation gate and quaternary amine inhibitors, Nature 411 (2001) 657–661.
[17] H.J.C. Berendsen, D. van der Spoel, R. van Drunen, GROMACS: a message—passing parallel molecular dynamics implementation, Comput. Phys. Commun. 91 (1995) 43–56.
[18] E. Lindahl, B. Hess, D. van der Spoel, Gromacs 3.0: a package for molecular simulation and trajectory analysis, J. Mol. Mod. 7 (2001) 306–317.
[19] Gromacs user manual version 3.0, Department of Biophysical Chemistry, University of Groningen, The Netherlands, 1991–2001, http://www.gromacs.org.
[20] H.J.C. Berendsen, J.P.M. Postma, A. DiNola, J.R. Haak, Molecular dynamics with coupling to an external bath, J. Chem. Phys. 81 (1984) 3684–3690.
[21] T. Darden, D. York, L. Pedersen, Particle mesh Ewald: an $N\cdot\log(N)$ method for Ewald sums in large systems, J. Chem. Phys. 98 (1993) 10089–10092.
[22] U. Essmann, L. Perera, M.L. Berkowitz, T. Darden, H. Lee, L.G. Pedersen, A smooth particle mesh Ewald method, J. Chem. Phys. 103 (1995) 8577–8593.
[23] O. Berger, O. Edholm, F.J. Jähnig, Molecular dynamics simulation of a fluid bilayer of dipalmitoylphosphatidylcholine at full hydration, constant pressure and constant temperature, Biophys. J. 72 (1997) 2002–2013.
[24] H.J.C. Berendsen, J.P.M. Postma, W.F. van Gunsteren, J. Hermans, in: B. Pullman Reidel (Ed.), Intermolecular Forces, Holland, Dordrecht, 1981, p. 331.

[25] S. Miyamoto, P.A. Kollman, SETTLE: an analytical version of the SHAKE and RATTLE algorithm for rigid water models, J. Comput. Chem. 13 (1992) 952–962.
[26] V.B. Luzhkov, J. Åqvist, A computational study of ion binding and protonation states in the KcsA potassium channel, Biochim. Biophys. Acta 1481 (2000) 360–370.
[27] S. Bernèche, B. Roux, The ionization state and conformation of Glu-71 int the KcsA K^+ channel, Biophys. J. 82 (2002) 772–780.
[28] C. Domene, A. Grottesi, M. Sansom, Filter flexibility and distortion in a bacterial inward rectifier K^+ channel: simulation studies of KirBac1.1, Biophys. J. 87 (2004) 256–267.
[29] Y. Zhou, R. MacKinnon, The occupancy of ions in the K^+ selectivity filter: charge balance and coupling of ion binding to a protein conformational change underlie high conduction rates, J. Mol. Biol. 333 (2003) 965–975.